Meteoritics & Planetary Science 40, Nr 11, 1563–1574 (2005)
Abstract available online at http://meteoritics.org

Radar observations of Itokawa in 2004 and improved shape estimation

Steven J. OSTRO[1*], Lance A. M. BENNER[1], Christopher MAGRI[2], Jon D. GIORGINI[1], Randy ROSE[1], Raymond F. JURGENS[1], Donald K. YEOMANS[1], Alice A. HINE[3], Michael C. NOLAN[3], Daniel J. SCHEERES[4], Stephen B. BROSCHART[4], Mikko KAASALAINEN[5], and Jean-Luc MARGOT[6]

[1]Jet Propulsion Laboratory, California Institute of Technology, Pasadena, California 91109–8099, USA
[2]University of Maine at Farmington, 173 High Street, Preble Hall, Farmington, Maine 04938, USA
[3]Arecibo Observatory, HC3 Box 53995, Arecibo, Puerto Rico 00612, USA
[4]Department of Aerospace, Engineering, University of Michigan, Ann Arbor, Michigan 48109–2140, USA
[5]Rolf Nevanlinna Institute, University of Helsinki, P.O. Box 4, FIN-00014 Helsinki, Finland, and Sodankyla Geophysical Observatory, University of Oulu, Tahtelantie 62, FIN-99600 Sodankyla, Finland
[6]Department of Astronomy, Space Sciences Building, Cornell University, Ithaca, New York 14853–6801, USA
*Corresponding author. E-mail: ostro@reason.jpl.nasa.gov

(Received 09 June 2005; revision accepted 21 September 2005)

Abstract–We present June 2004 radar images of asteroid 25143 Itokawa (1998 SF36) that improve upon the longitude-latitude coverage of images obtained in 2001 by Ostro et al. (2004) and use the 2001–2004 data to refine that paper's constraints on Itokawa's shape. The 2004 images, the first of the asteroid's southern side, look distinctly different from the 2001 images, revealing leading edges that are much more curved and rugged than the nearly convex leading edges seen at northern latitudes in 2001. Itokawa is shaped like a slightly asymmetrical, bent, lumpy ellipsoid with dimensions along the principal axes within 10% of 594 × 320 × 288 m. To illustrate the uncertainty space associated with shape reconstruction from images with suboptimal orientational coverage, we present two alternative three-dimensional models of the object.

INTRODUCTION

Ostro et al. (2004) reported delay-Doppler radar observations of Itokawa during March-April 2001 and presented a preliminary reconstruction of Itokawa's shape from images with extremely limited orientational coverage, using the method of Hudson (1993) and adopting the lightcurve-derived spin period (P = 12.132 h) and pole direction (ecliptic long., lat. = 355°, –84°) obtained by Kaasalainen et al. (2003). The rationale for publishing this preliminary model was to assist the Hayabusa (MUSES-C) project in planning its rendezvous and sampling operations.

The subradar tracks of the highest-resolution images obtained in 2001 were confined to a narrow band of northern, temperate latitudes and less than 40% of a rotation. As stressed by Ostro et al. (2004), the 2001 images with both high SNR and high resolution were restricted to a very narrow latitude-longitude region. Accurate definition of an asteroid's pole-on silhouette (or the silhouette's convex hull) requires at least 180° of rotation phase coverage by the radar images (Ostro et al. 1988). Accurate reconstruction of the three-dimensional shape additionally requires latitude coverage at least a few tens of degrees from the equator to break the delay-Doppler projection's intrinsic north-south ambiguity. For Itokawa, with its half-day period, obtaining wide longitude coverage at high SNR in 2001 was difficult. The Arecibo images were stronger than the Goldstone images but were limited in longitude coverage by Arecibo's short hour-angle window, while the Goldstone images achieved wider longitude coverage but were much lower-SNR than the Arecibo images. Since the close approach occurred at declinations favorable to Arecibo, the best Arecibo images sampled the same latitudes as the best Goldstone images.

In June 2004, we conducted Goldstone and Arecibo observations of Itokawa with subradar tracks that span latitudes from –13° to –27° and 3/4 of a rotation. The 2004 images, the first of the asteroid's southern side, look distinctly different from the 2001 images. While the 2001 images showed a nearly ellipsoidal shape devoid of noteworthy topographic relief, the 2004 images are replete with intriguing topographic structure. Dark portions of many images suggest subtle concavities, and the irregularity of many images' trailing edges suggests structure at several-

© The Meteoritical Society, 2005. Printed in USA.

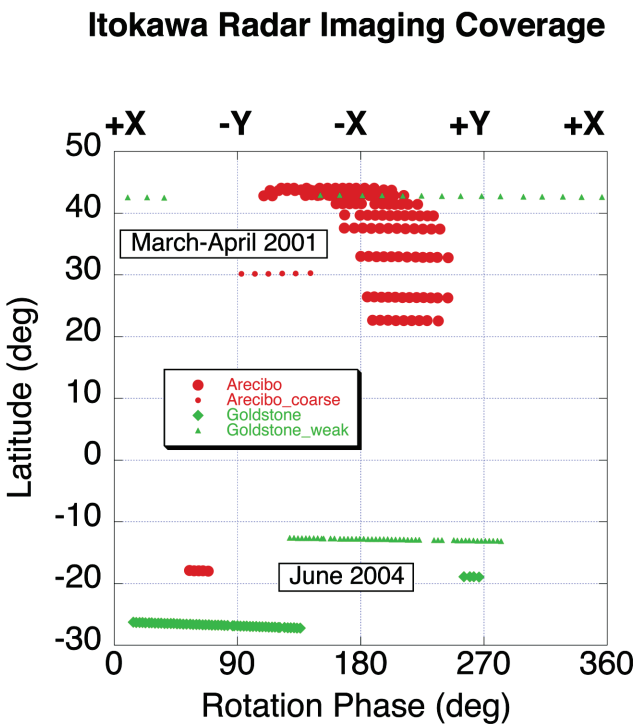


Fig. 1. Arecibo (red) and Goldstone (green) subradar locations of the delay-Doppler images used to estimate Itokawa'shape. Rotation is about the model's shortest principal axis (z). The +x axis passes through the zero meridian. Rotation phase (west longitude) increases as the asteroid rotates, and the succession of radar-facing longitudes proceeds in the order +x, –y, –x, +y, as indicated at the top. The northern tracks are from 2001 and the southern tracks are from 2004 (see Table 1). The larger symbols indicate the higher-SNR, finer-resolution data. The 2001 Mar. 18 Arecibo track (small red symbols) used a very coarse-resolution setup. The 2001 Mar. 30 Goldstone track (upper small green symbols) was much weaker than any of the 2001 Arecibo tracks. The 2004 Jun. 17–18 track (lower small green symbols) was much lower-SNR than any of the other data sets used in our estimation.

decameter scales. The object's leading edges seen at southern subradar latitudes in 2004 are much more curved and rugged than the nearly convex leading edges seen at northern latitudes in 2001. Although Itokawa's topography is not excessive, it certainly is not as subtle as it appeared to be from the 2001 investigation.

In 2004, Itokawa's radar-accessible approach was closer than that in 2001, so Goldstone obtained stronger echoes than in 2001. The improved longitude coverage plus the visibility of southern latitudes in 2004 has produced a 2001 + 2004 data set of high-SNR radar images that has significantly more geometric leverage for reconstructing Itokawa's shape than the 2001 data set alone, despite the much smaller number of observing dates in 2004. We have used our 2001 and 2004 data in combination with the Kaasalainen et al. (2004) improved spin vector (P = 12.13237 + 0.00008 h, J2000 ecliptic long., lat. = 330°, –89° ± 5°) to improve our constraints on Itokawa's three-dimensional shape.

Table 1 gives information about the 2001 and 2004 radar data sets used in our modeling, and Fig. 1 shows their subradar locations. Because the accuracy of a radar-based shape reconstruction relies on the completeness of subradar longitude and latitude coverage, we forewarn readers that despite the expanded longitude-latitude coverage of the 2001 + 2004 data set, we still are concerned about the data set's limitations, for the following reasons. (Note the smaller symbols in Fig. 1 and the columns giving signal-to-noise ratio and subradar latitude in Table 1.) All the Arecibo sequences are strong, but the first (2001 March 18) is at very coarse resolution. The 2001 March 30 Goldstone data are much weaker than any of the Arecibo tracks, and the 2004 June 17–18 Goldstone images, obtained at a greater distance from Itokawa than any of the other 2004 images, are extremely weak. We have omitted other Goldstone tracks because they are either far too weak to be useful or because they are weak and provide redundant subradar coverage, but we retain those two Goldstone tracks because of their unique coverage.

MODELING TECHNIQUE

We used Hudson's (1993) technique and software developed by him to estimate Itokawa's shape, as described in Hudson and Ostro (1994, 1995), Hudson et al. (2000), and Ostro et al. (2002, 2004). We initially assumed a pole direction, (330°, –89°), based on the Kaasalainen et al. (2004) analysis of 2001–2004 optical lightcurves, which is 5° from the Kaasalainen et al. (2003) pole, (335°, –84°), and a sidereal rotation period P = 12.13237 h. Our estimations included experiments in which we treated the spin vector's direction and/or magnitude as free parameters, but our results support the Kaasalainen et al. (2004) results.

Our estimations started with an ellipsoid model and proceeded first to a spherical harmonics model (in which surface displacement is expressed as a truncated spherical harmonic expansion) and then to a vertex model. In each case we adjusted the free parameters to optimize the resemblance of images synthesized from the shape model to our radar images. The fits included parameters for the asteroid's shape and spin state, the radar scattering law, the radar system calibration, and corrections to the ephemeris predictions of the delay-Doppler location of the center of mass (COM) in each frame.

In the Hudson SHAPE software, ellipsoid models, "harmonic" models, and vertex models are all realized as polyhedra with triangular sides. (A triangular-faced polyhedron with V vertices has $2V$–4 faces and $3V$–6 edges.) The user controls the value of V in a realization. Larger values of V provide greater spatial resolution and, for ellipsoid and harmonic models, sample the mathematical function more densely, but they also slow the estimation.

SHAPE minimizes an objective function that consists of the weighted sum of: i) the squared residuals between delay-

Table 1. Observations. This table gives information about the delay-Doppler images used in our modeling: a total of 258 frames organized by date and/or receiver setup into 19 data sets. For each set, we give the range of receive start times, the orbit solution number for the delay-Doppler prediction ephemeris produced by JPL's On-Site Orbit Determination program (OSOD), the delay-Doppler resolution, the number of frames, the average number of independent looks per frame, the average echo signal-to-noise ratio per frame, Itokawa's right ascension, declination, and distance, and the subradar latitude.

Data set	A/G	Year	Month	Day	RCV start (hhmmss-hhmmss)	Orbit solution	Delay resolution (μs)	Doppler resolution (Hz)	Number of frames	Avg. looks per frame	Avg. SNR per frame	RA, dec.	Distance (AU)	Lat. (deg)
0	A	2001	Mar	18	060716–074916	30	0.500	0.060	6	30	98	208°, 20°	0.060	30°
1	A	2001	Mar	26	073447–091149	42	0.100	0.065	5	8	180	242°, 23°	0.041	43°
2	A	2001	Mar	27	074458–095716	42	0.100	0.065	12	18	260	248°, 22°	0.039	44°
3	A	2001	Mar	28	080059–101654	44	0.100	0.065	12	14	220	254°, 22°	0.039	44°
4	A	2001	Mar	29	082924–104124	48	0.100	0.065	12	18	260	261°, 21°	0.038	44°
5	A	2001	Mar	30	084427–105907	50	0.100	0.065	12	18	280	267°, 20°	0.038	43°
6	A	2001	Mar	31	092015–111943	50	0.100	0.065	12	15	230	273°, 18°	0.039	42°
7	A	2001	Apr	1	093421–114414	50	0.100	0.065	12	16	220	279°, 17°	0.040	40°
8	A	2001	Apr	2	093640–115702	50	0.100	0.065	12	18	210	284°, 15°	0.041	38°
9	A	2001	Apr	4	101125–121955	50	0.100	0.065	12	15	144	294°, 12°	0.044	33°
10	A	2001	Apr	7	104548–124428	52	0.100	0.065	12	13	74	305°, 8°	0.051	26°
11	A	2001	Apr	9	111423–125124	52	0.100	0.065	9	13	63	311°, 6°	0.057	23°
12	G	2001	Mar	30	085641–170849	50	0.125	0.250	18	127	33	268°, 19°	0.038	43°
13	A	2004	Jun	19	185035–191808	107	0.100	0.050	5	7	120	122°, 2°	0.028	–18°
14	G	2004	Jun	17	204606–215141	107	0.125	0.250	12	35	28	124°, 6°	0.034	–13°
15	G	2004	Jun	17	220012–235725	107	0.125	0.250	21	35	28	124°, 6°	0.034	–13°
16	G	2004	Jun	18	001848–015742	107	0.125	0.250	16	35	28	123°, 6°	0.033	–13°
17	G	2004	Jun	20	013604–015807	107	0.125	0.250	4	34	58	122°, 1°	0.027	–19°
18	G	2004	Jun	21	180034–220723	107	0.125	0.250	54	30	96	119°, –7°	0.022	–27°

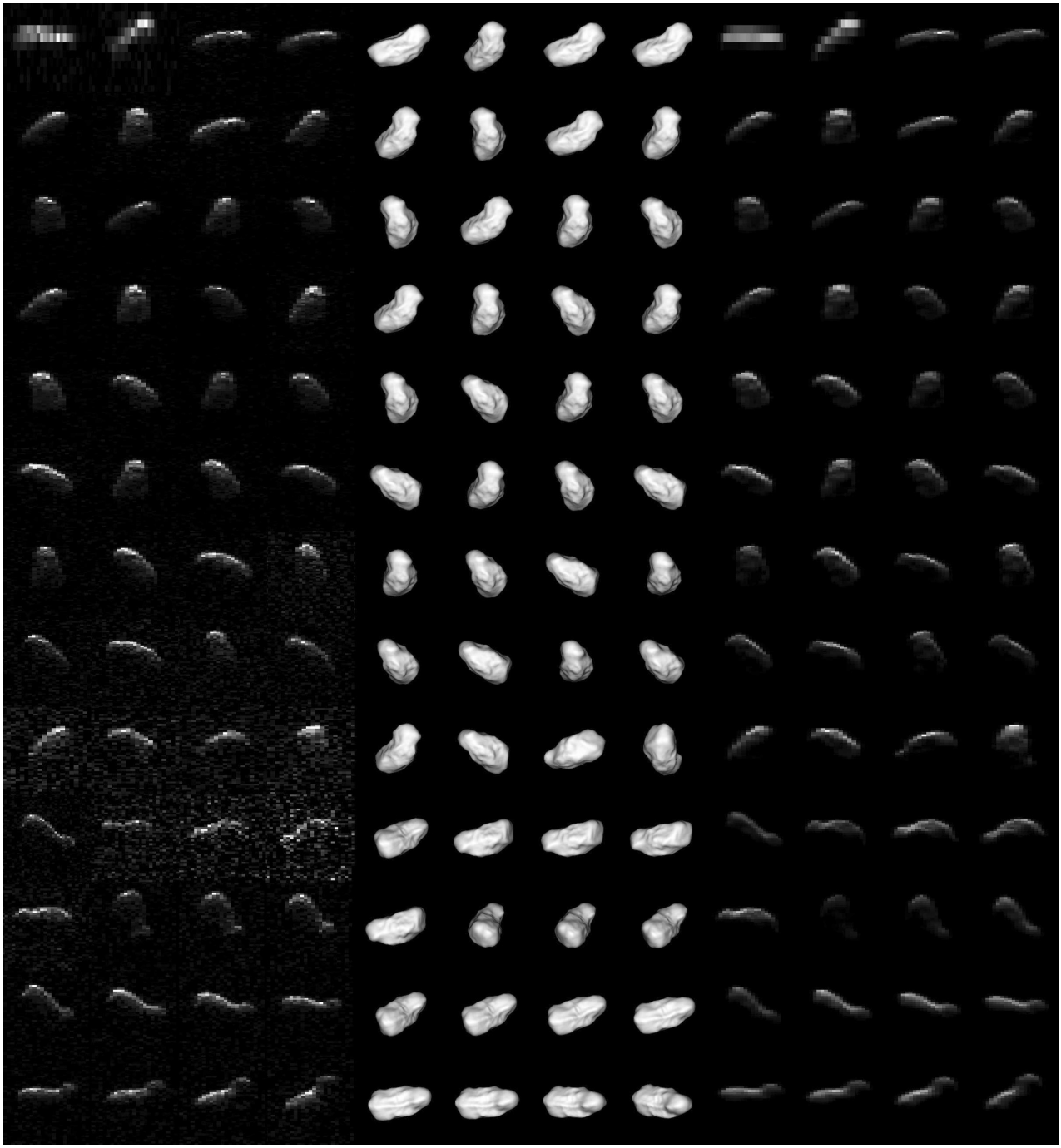


Fig. 2a. Results for our Itokawa-2005-Rough model. Each of the three vertical panels contains 52 frames. The left panel shows data images, the right panel shows corresponding "fit" images synthesized from our model, and the middle panel shows plane-of-sky renderings of a smoothed version of the shape model (Table 2), with north upward and east leftward. The 52 frames are arranged chronologically (left to right in the first row, etc.) and include every fifth imaging frame on each observation date used in our modeling except for the very weak 2004 Jun. 17–18 data. Whereas the overall match between observed and fit images looks decent for most frames, we do not consider the fits to certain frames to be satisfactory. This situation probably reflects a combination of the complexity of the asteroid's shape visible in those images and the suboptimal orientational coverage.

Doppler image pixel values and the corresponding values predicted by the physical model and ii) penalty functions that can be adjusted to suppress structural features. We experimented with weights applied to penalty functions that enforce principal-axis rotation and uniform density distribution, finding no convincing evidence that relaxing these conditions improved the fits; that is, our results are consistent with Itokawa being a uniform-density, principal-

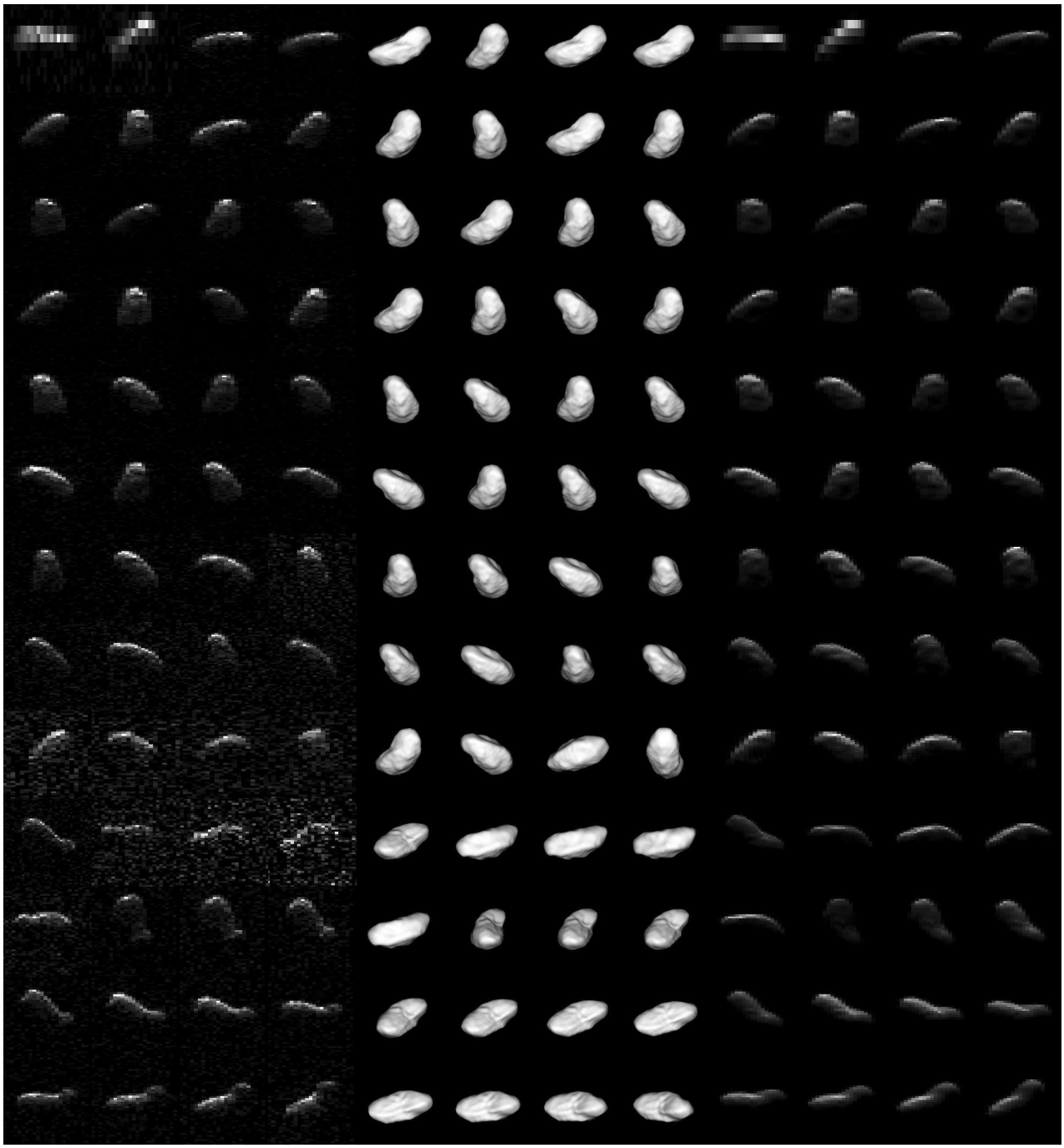


Fig. 2b. Results for our Itokawa-2005-Smooth model. Each of the three vertical panels contains 52 frames. The left panel shows data images, the right panel shows corresponding "fit" images synthesized from our model, and the middle panel shows plane-of-sky renderings of a smoothed version of the shape model (Table 2), with north upward and east leftward. The 52 frames are arranged chronologically (left to right in the first row, etc.) and include every fifth imaging frame on each observation date used in our modeling except for the very weak 2004 Jun. 17–18 data. Whereas the overall match between observed and fit images looks decent for most frames, we do not consider the fits to certain frames to be satisfactory. This situation probably reflects a combination of the complexity of the asteroid's shape visible in those images and the suboptimal orientational coverage.

axis rotator. We also penalized structural relief, trying to strike a balance between allowing sufficient structure to reproduce the appearance of the images and suppressing structure that is not geologically plausible.

The shape estimation process depends critically on initial conditions, because the problem is highly nonlinear and the parameter space (and hence the chi-square hypersurface) is huge and complex. The initial conditions include starting

Table 2.

		Rough	Smooth	Adopted
Extents along principal axes	x	590	598	594 ± 10%
	y	323	317	320 ± 10%
	z	310	276	288 ± 10%
Extent ratios	x/y	1.81	1.89	1.85 ± 15%
	y/z	1.08	1.15	1.11 ± 15%
Area (km^2)	0.497	0.468	0.482 ± 20%	
Volume (km^3)	0.0263	0.0238	0.025 ± 30%	
Ratios of the principal moments of inertia of a uniform-density asteroid with the model's shape	Iz/Ix	2.80	3.08	2.94 ± 20%
Equivalent diameter of a sphere with the model's volume		369	357	363 ± 10%
Dimensions of the dynamically equivalent equal-volume ellipsoid (DEEVE, the homogeneous ellipsoid having the same moment-of-inertia ratios and volume as the model)	x	613	613	613 ± 10%
	y	290	291	291 ± 10%
	z	282	255	268 ± 10%
Gravitational slope statistics for an assumed uniform density of 2.3 g/cm^3	Maximum	42°	41°	42° ± 10%
	Average	14°	13°	14° ± 10%
Angular scattering law exponent		2.28	2.18	2.23 ± 10%
OC radar albedo	Average	0.133	0.140	0.138 ± 10%
	r.m.s.	0.019	0.020	
Goodness-of-fit statistics				
Radar root-reduced chi-square with *actual* image weights		1.40	1.38	
Radar root-reduced chi-square with *equal* image weights		1.68	1.64	
Lightcurve r.m.s. deviation (magnitudes)		0.058	0.054	

values for parameters (e.g., the dimensions of the ellipsoid, the spin vector, and the radar scattering law), the length of the spherical harmonics expansion, the step sizes for iterations, the values of penalty function weights, and the number of vertices in each model realization. Furthermore, since some structure is seen only in relatively few of our data images, it is necessary to experiment with raising the relative weights of particular images so as to compensate for this, so images synthesized from the resultant model more closely resemble the data images. Finally, delay-Doppler images are time exposures, and a combination of coherent and incoherent summation (Ostro et al. 2002) is required to strike a balance between reducing rotational smearing and reducing the combination of receiver noise and echo self noise in the images. Thus there is an extremely strong subjective element in the estimation process.

MODELING RESULTS

After exhaustively exploring the estimation's effective overall parameter space, we conclude that the available data are inadequate to define the asteroid's shape as accurately as we would have liked, and certainly less adequate than previously published radar shape models. On the other hand, we think our results do reproduce Itokawa's primary qualitative and quantitative shape characteristics.

We have chosen to present two alternative models of Itokawa, Itokawa-2005-Rough and Itokawa-2005-Smooth, which we refer to as our rough and smooth models; as noted below, we prefer the latter. In generating any shape model, we gradually adjust the penalty weights and the relative image weights as we proceed from ellipsoid to harmonic to vertex models, seeking to guide the process so as to achieve the best possible fit. One such sequence of adjustments led to our rough model, while a different sequence resulted in our smooth model.

Table 2 gives salient characteristics of each model as well as our adopted consensus values and their assigned standard errors. Figure 2 shows about one-fifth of our 258 data frames, corresponding "fit" images synthesized from the models, and corresponding plane-of-sky (POS) renderings of smoothed versions of the models; movies showing all 258 frames are available at http://reason.jpl.nasa.gov/~ostro/ito_2005/Itokawa-2005-Rough.mov; http://reason.jpl.nasa.gov/~ostro/ito_2005/Itokawa-2005-Smooth.mov. The digital models in Wavefront "object" format are available at http://reason.jpl.nasa.gov/~ostro/ito_2005/Itokawa-2005-Rough.obj; and http://reason.jpl.nasa.gov/~ostro/ito_2005/Itokawa-2005-Smooth.obj.

Figure 3 shows principal-axis projections of smoothed renderings of the models. Figure 4 shows principal-axis projections of unsmoothed renderings of the models that are color-coded for gravitational slope (the angle which a plumb line would make with the local normal to the surface) under

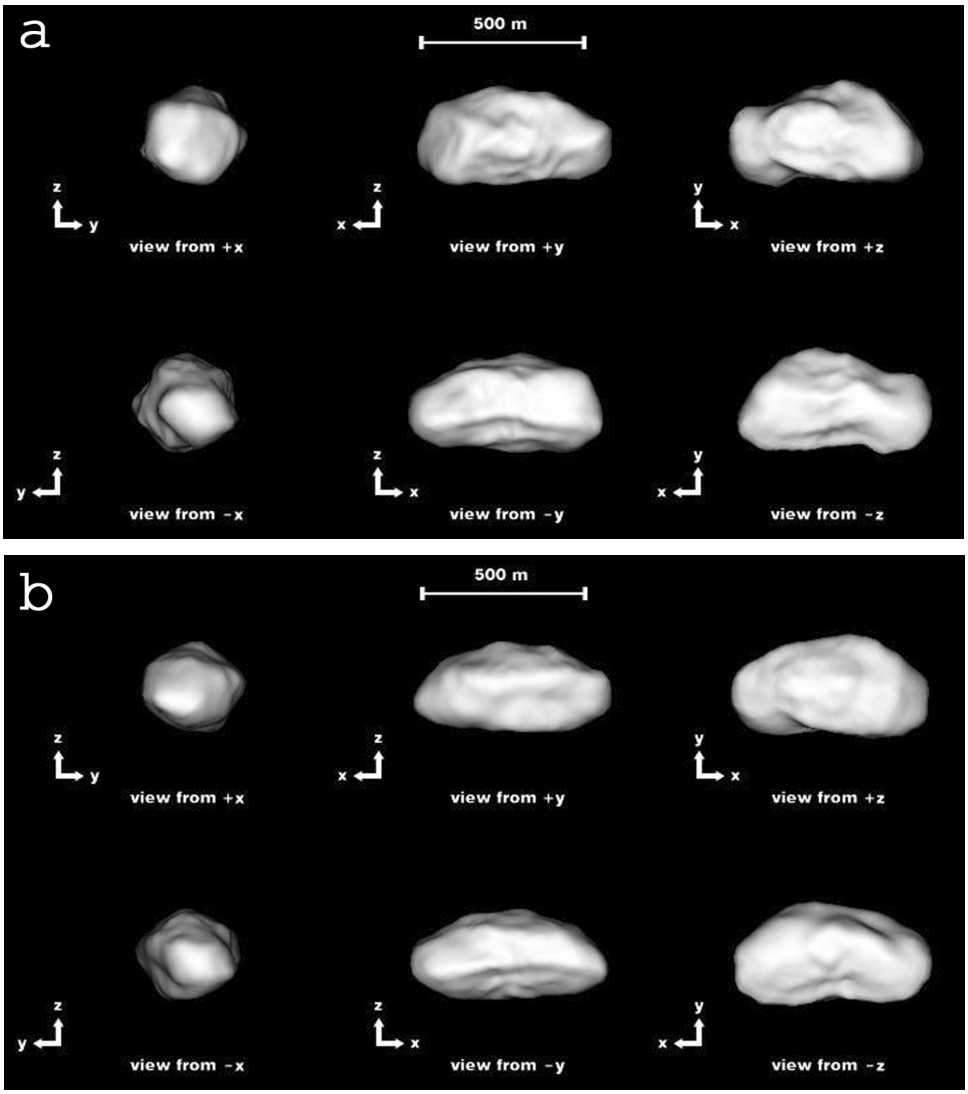


Fig. 3. Renderings of smoothed versions of: a) our Itokawa-2005-Rough model and b) our Itokawa-2005-Smooth model (Table 2) viewed along the principal-axis directions.

the assumption of uniform density and taking into consideration the asteroid's rotation. The finest imaging resolution and the typical edge length of our polyhedral models are between one and two decameters, and the intrinsic reconstruction uncertainty is about 30 m.

Itokawa is shaped like a slightly asymmetrical, bent, lumpy ellipsoid with dimensions along the principal axes within 10% of 594 × 320 × 288 m. The rough model has a slightly longer polar axis, which translates into slightly larger model area and volume.

There is a concavity on the asteroid's –y side that is easily seen in the views along the +z and –z axes in Figs. 3 and 4. The concavity is not a crater, but might be described as a saddle. Both models have a concavity on the +y side, north of the equator, but its topology on our rough model gives the impression of there being a neck that defines the –x end as a sort of knob. The rough model's gravitational slopes on this neck are among the steepest on the object. The smooth model's concavities and slopes are more subdued than the rough model's counterparts.

The knob, seen on the right side of the object in the last frames in Figs. 2a and 2b, is more pronounced than it appears.in either model. Also, the concavity adjacent to it, revealed on the leading edge of the Jun. 21 (Set 18) images, is deeper than suggested by either model, although the rough model reproduces it better. Thus, some of Itokawa's topographic structure that is evident in the images is incompletely reproduced in our models. Conversely, it is possible that some of the models' topography, such as the ridge-like structure seen along much of the length of the asteroid in the views from –y in Fig. 3 and Fig. 4, might be an artifact of the modeling process, possibly reflecting either insufficient high-latitude coverage to overcome the images' north-south ambiguity or our choices of penalty weights. The

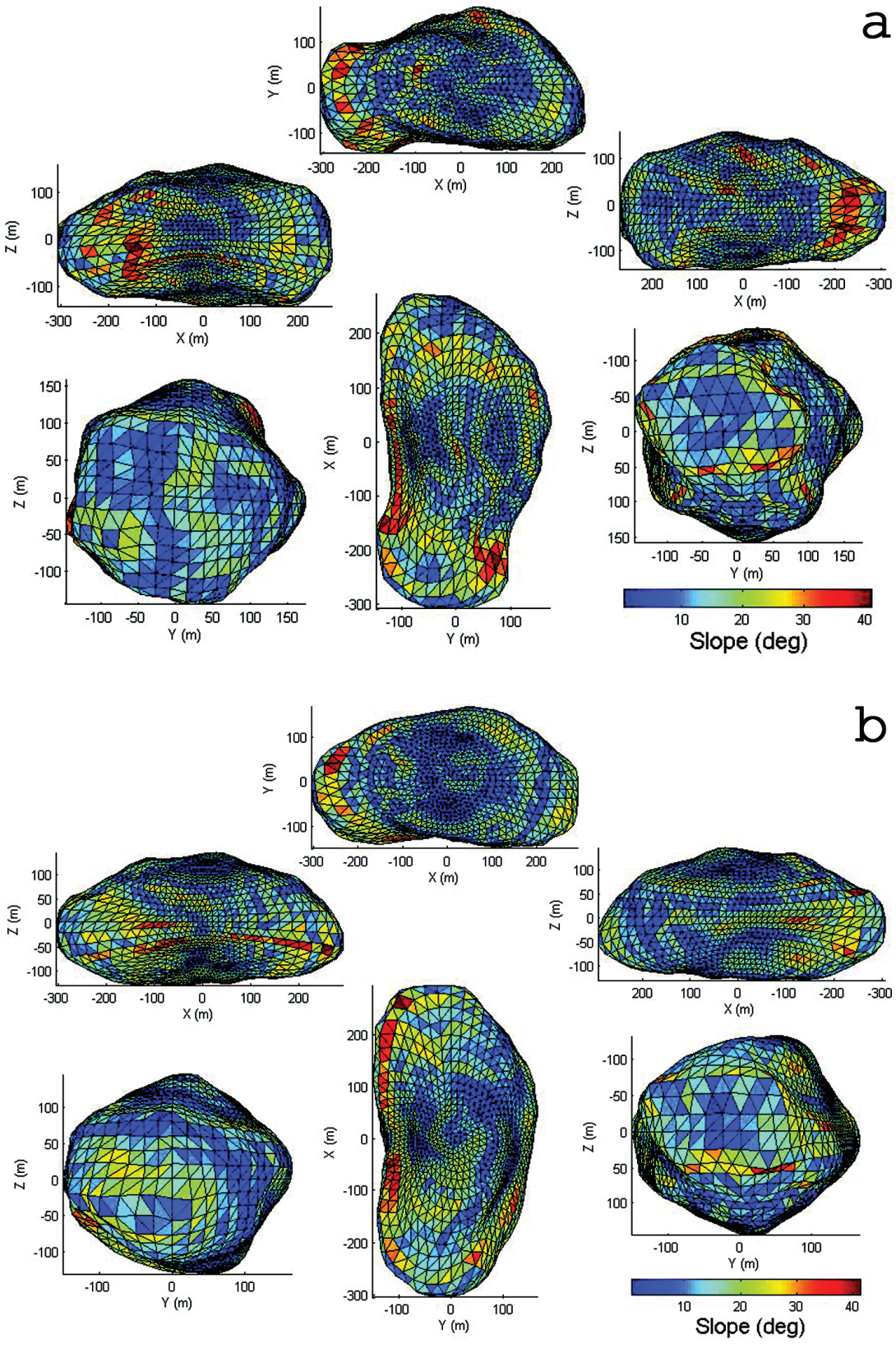


Fig. 4. Renderings of unsmoothed versions of a) our Itokawa-2005-Rough model and b) our Itokawa-2005-Smooth model (Table 2) viewed along the principal-axis directions and color-coded for gravitational slope in degrees.

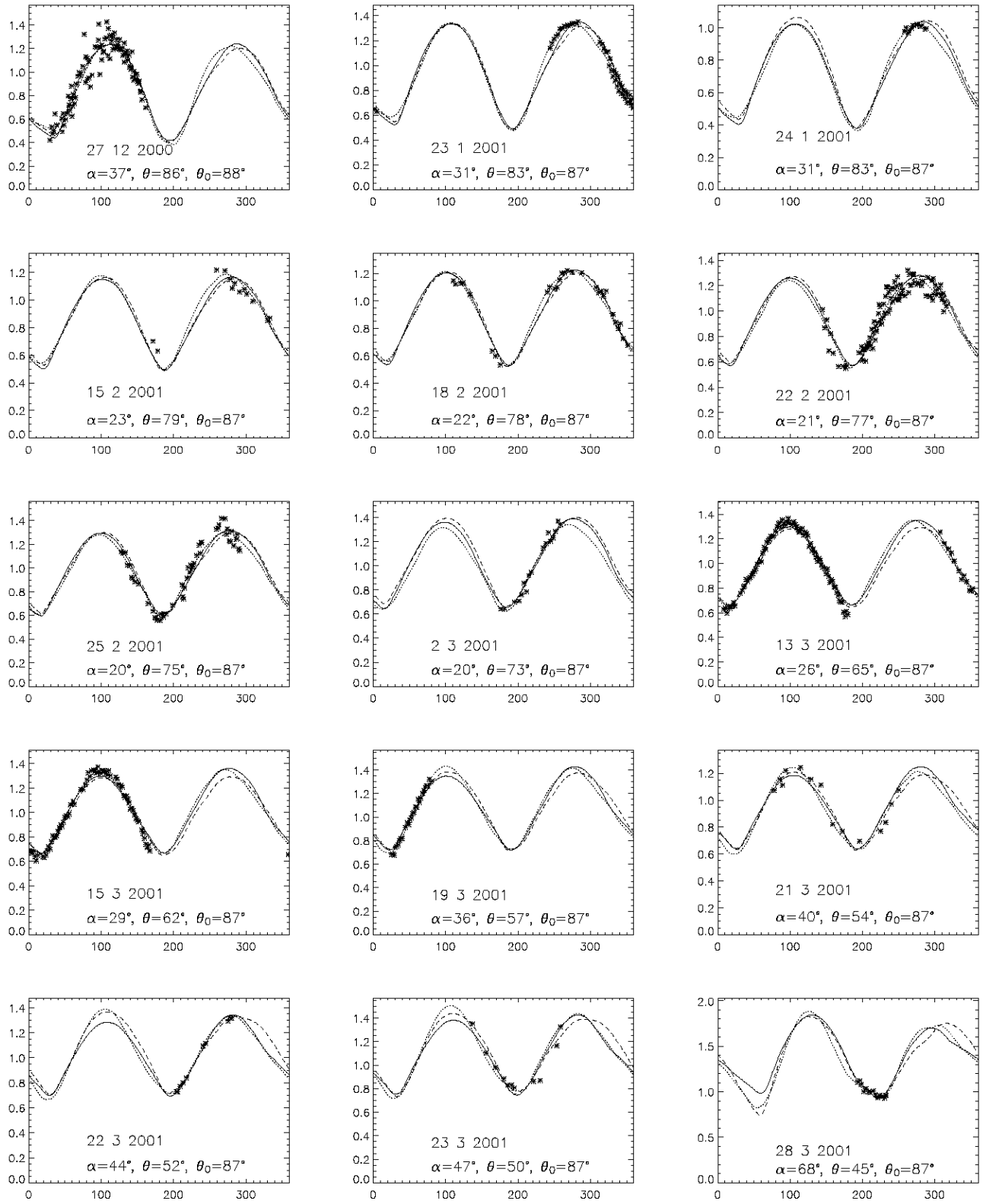


Fig. 5. Itokawa 2001 and 2004 lightcurves (asterisks) and the corresponding fits for the smooth radar model (solid curves), the rough radar model (dashed curves) and the Kaasalainen et al. (2005) lightcurve inversion (dotted curves). The horizontal axes give the rotational phase in degrees, and the vertical axes give brightness in units of relative intensity. Each plot is labeled with the solar phase angle (α), the aspect angle (θ, from the pole to the line of sight), and the illumination angle (θ_0, from the pole to the asteroid-sun line). Optical lightcurves synthesized from our models provide better fits to Itokawa photometry than the preliminary model of Ostro et al. (2004).

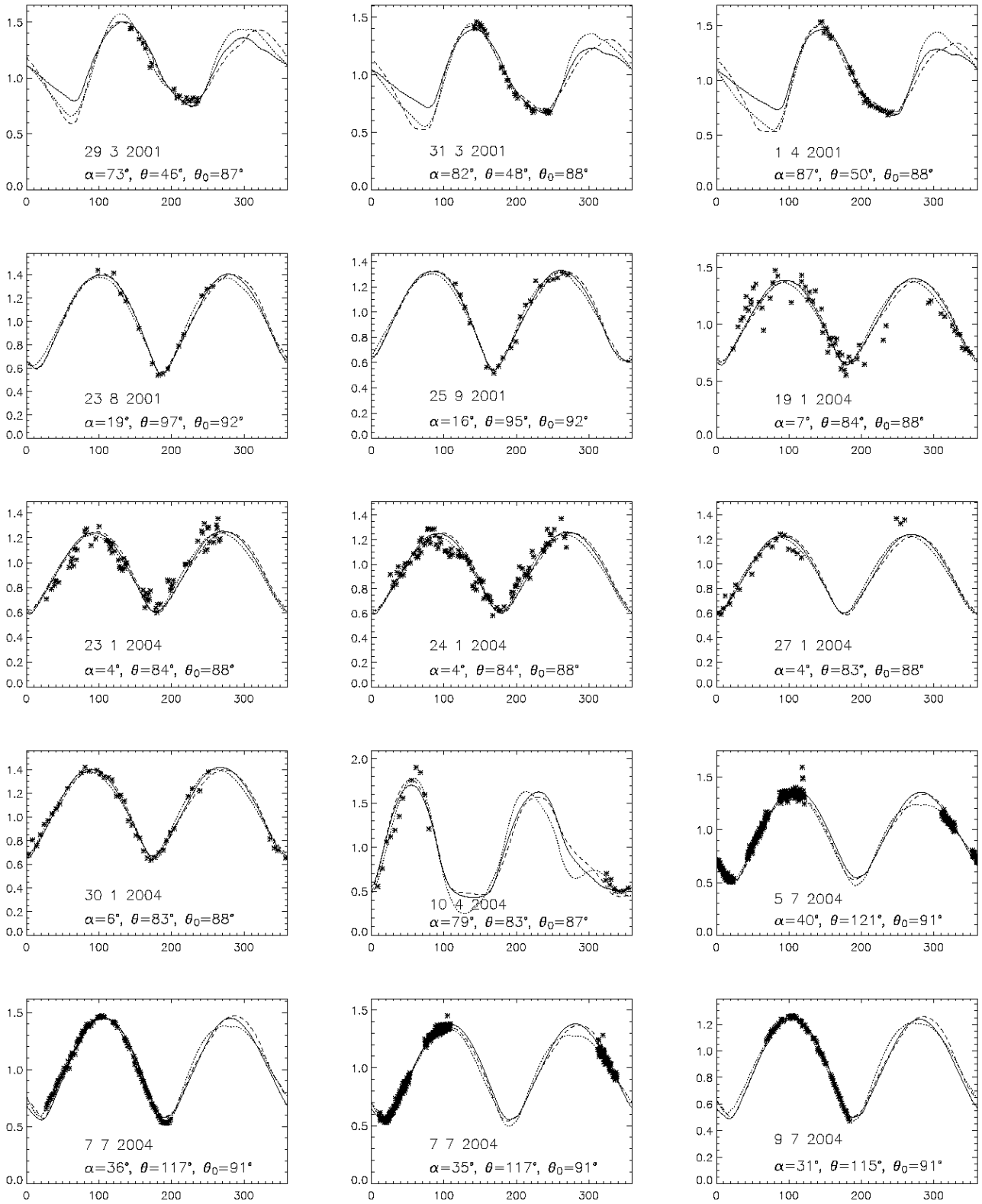


Fig. 5. *Continued*. Itokawa 2001 and 2004 lightcurves (asterisks) and the corresponding fits for the smooth radar model (solid curves), the rough radar model (dashed curves) and the Kaasalainen et al. (2005) lightcurve inversion (dotted curves). The horizontal axes give the rotational phase in degrees, and the vertical axes give brightness in units of relative intensity. Each plot is labeled with the solar phase angle (α), the aspect angle (θ, from the pole to the line of sight), and the illumination angle (θ_0, from the pole to the asteroid-sun line). Optical lightcurves synthesized from our models provide better fits to Itokawa's photometry than the preliminary model of Ostro et al. (2004).

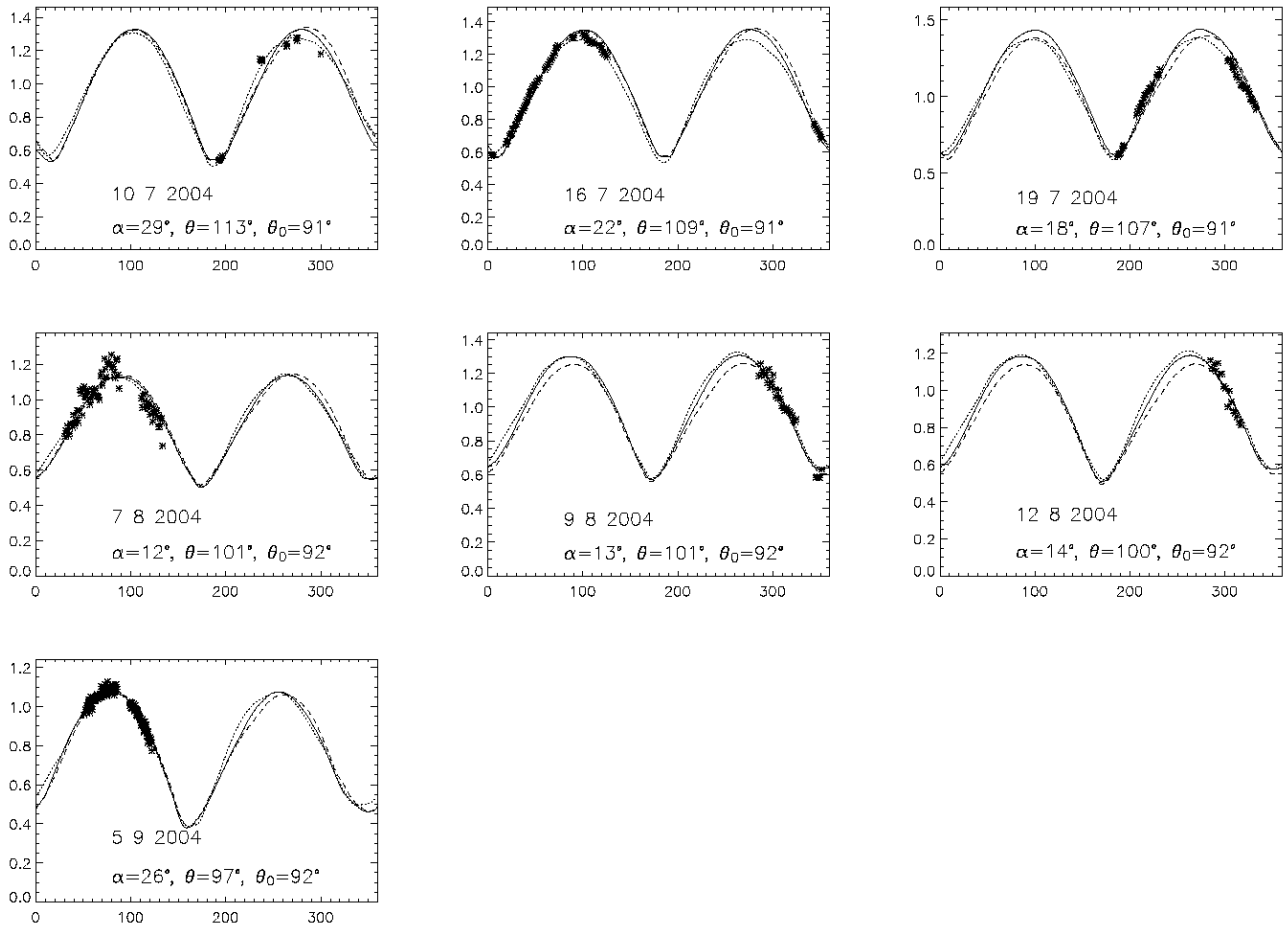


Fig. 5. *Continued*. Itokawa 2001 and 2004 lightcurves (asterisks) and the corresponding fits for the smooth radar model (solid curves), the rough radar model (dashed curves) and the Kaasalainen et al. (2005) lightcurve inversion (dotted curves). The horizontal axes give the rotational phase in degrees, and the vertical axes give brightness in units of relative intensity. Each plot is labeled with the solar phase angle (α), the aspect angle (θ, from the pole to the line of sight), and the illumination angle (θ_0, from the pole to the asteroid-sun line). Optical lightcurves synthesized from our models provide better fits to Itokawa photometry than the preliminary model of Ostro et al. (2004).

goodness-of-fit statistics in Table 2 quantify the limited accuracy of our models. The smooth model is favored by those statistics and by the fits to optical lightcurves (Fig. 5), although some radar image frames seem better reproduced by the rough model.

The lightcurve inversion model of Kaasalainen et al. (2005) portrays global shape characteristics consistent with those of the radar models presented here. It is interesting that the lightcurve model and both radar models have different predictions for those sections of March-April 2001 lightcurves for which there are no data.

CONCLUSION

We take the smooth model our more accurate estimate, with an uncertainty defined by the difference between it and the rough model. We look forward to Hayabusa's imaging of Itokawa, which will help us assess the accuracy of shape estimation using Hudson's technique in situations with suboptimal orientational coverage by a radar data set. It also will let us compare the merits of inferences about physical properties from radar images versus disc-integrated techniques.

Acknowledgments–We thank Scott Hudson for providing his shape reconstruction software. We thank the technical staffs at Arecibo and Goldstone for help with the observations. Some of our Arecibo observations used the CalTech Baseband recorder (CBR), whose development and fabrication was funded by the National Science Foundation. S. J. Ostro was partially supported by the JPL MUSES-C Project and the Steven and Michele Kirsch Foundation. D. J. Scheeres was partially supported by NASA's Planetary Geology and Geophysics program. C. Magri was partially supported by NSF grant AST-0205975. J. L. Margot was partially supported by NASA's Planetary Astronomy program. Part of this research was conducted at the Jet Propulsion Laboratory, California Institute of Technology, under contract with the

National Aeronautics and Space Administration (NASA). The Arecibo Observatory is part of the National Astronomy and Ionosphere Center, which is operated by the Cornell University under a cooperative agreement with the National Science Foundation.

Editorial Handling—Dr. Walter Huebner

REFERENCES

Hudson S. 1993. Three-dimensional reconstruction of asteroids from radar observations. *Remote Sensing Reviews* 8:195–203.

Hudson R. S. and Ostro S. J. 1994. Shape of asteroid 4769 Castalia (1989 PB) from inversion of radar images. *Science* 263:940–943.

Hudson R. S., and Ostro S. J. 1995. Shape and spin state of asteroid 4179 Toutatis from radar images. *Science* 270:84–86.

Hudson R. S., Ostro S. J., Jurgens R. F., Rosema K. D., Giorgini J. D., Winkler R., Rose R., Choate D., Cormier R. A., Franck C. R., Frye R., Howard D., Kelley D., Littlefair R., Slade M. A., Benner L. A. M., Thomas M. L., Mitchell D. L., Chodas P. W., Yeomans D. K., Scheeres D. J., Palmer P., Zaitsev A., Koyama Y., Nakamura A., Harris A. W., and Meshkov M. N. 2000. Radar observations and physical modeling of asteroid 6489 Golevka. *Icarus* 148:37–51.

Ostro S. J., Hudson R. S., Benner L. A. M., Giorgini J. D., Magri C., Margot J.-L., and Nolan M. C. 2002. Asteroid radar astronomy. In *Asteroids III*, edited by Bottke W. F. Jr., Cellino A., Paolicchi P., and Binzel R. P. Tucson: The University of Arizona Press. pp. 151–168.

Kaasalainen M., Kwiatkowski T., Abe M., Piironen J., Nakamura T., Ohba Y., Dermawan B., Farnham T., Colas F., Lowry S., Weissman P., Whiteley R. J., Tholen D. J., Larson S. M., Yoshikawa M., Toth I., and Velichko F. P. 2003. CCD photometry and model of MUSES-C target (25143) 1998 SF36. *Astronomy & Astrophysics* 405:L29–L32.

Kaasalainen M., Masanao A., Byron J., Delbo M., DiMartino M., Higgins D., Kitazato K., Lowry S., Masi G., Mueller M., Naranen J., Vokrouhlicky' D., Warner B. D., Weissman P., and Young P. Forthcoming. Photometric observations 2001–2004 and modelling of (25143) Itokawa. Proceedings, 1st Hayabusa Symposium.

Ostro S. J., Connelly R., and Belkora L. 1988. Asteroid shapes from radar echo spectra: A new theoretical approach. *Icarus* 73:15–24.

Ostro S. J., Benner L. A. M., Nolan M. C., Magri C., Giorgini J. D., Scheeres D. J., Broschart S. B., Kaasalainen M., Vokrouhlicky' D., Chesley S. R., Margot J. L., Jurgens R. F., Rose R., Yeomans D. K., Suzuki S., and De Jong E. M. 2004. Radar observations of asteroid 25143 Itokawa (1998 SF36). *Meteoritics & Planetary Science* 39:407–424.